

Modelling and optimization of an innovative facility for automated sorting of aluminium scraps

Wu, Yongli; Oudshoorn, Tijmen; Rem, Peter

DOI

10.1016/j.wasman.2024.08.018

Publication date

Document Version Final published version

Published in Waste Management

Citation (APA)
Wu, Y., Oudshoorn, T., & Rem, P. (2024). Modelling and optimization of an innovative facility for automated sorting of aluminium scraps. Waste Management, 189, 103-113. https://doi.org/10.1016/j.wasman.2024.08.018

Important note

To cite this publication, please use the final published version (if applicable). Please check the document version above.

Copyright

Other than for strictly personal use, it is not permitted to download, forward or distribute the text or part of it, without the consent of the author(s) and/or copyright holder(s), unless the work is under an open content license such as Creative Commons.

Please contact us and provide details if you believe this document breaches copyrights. We will remove access to the work immediately and investigate your claim.

ELSEVIER

Contents lists available at ScienceDirect

Waste Management

journal homepage: www.elsevier.com/locate/wasman



Research Paper



Modelling and optimization of an innovative facility for automated sorting of aluminium scraps

Yongli Wu^{a,*}, Tijmen Oudshoorn^b, Peter Rem^a

- ^a Faculty of Civil Engineering and Geosciences, Delft University of Technology, Delft 2628 CN, the Netherlands
- ^b Myne Circular Metals, Harderwijk 3846 BP, the Netherlands

ARTICLE INFO

Keywords: Aluminium recycling Aluminium scraps Scrap sorting technology DEM Virtual experiment model Circularity

ABSTRACT

The growing demand for aluminium worldwide makes aluminium recycling critical to realising a circular economy and increasing the sustainability of our world. One effective way to improve the impact of aluminium recycling is to develop cost-efficient automated sorting technologies for obtaining pre-defined high-quality aluminium scrap products, thus reducing undesirable downcycling and increasing environmental/economic benefits. In this work, an innovative facility, which includes singulation, sensor scanning, and ejection, is optimised for the automated sorting of aluminium scraps. The sorting facility is computationally studied by a virtual experiment model based on the discrete element method. The model considers particle-scale dynamics of complex-shaped scraps and mimics the automated operation of the facility. Based on virtual experiment modelling, the flow of scrap is optimized by computation, with the feasible operation of the sorting facility being proposed. Accordingly, the sorting facility has been built and model predictions are confirmed in actual operation.

1. Introduction

Aluminium is the most widely used non-ferrous metal worldwide, and its global demand is expected to continually grow over the 21st century (Watari et al., 2021). To meet its increasing demand and reduce the corresponding impacts of resource consumption and pollutant emissions, the secondary production of aluminium from waste recycling is expected to play an increasingly important role (Soo et al., 2018; Van der Voet et al., 2018; Aluminium, 2019). In the aluminium recycling process, end-of-life products are shredded to scraps within a welldefined size range and these are sorted into groups before subsequent processing. Depending on the processing capability of the recycling plants and/or the economic benefits, aluminium scraps can be sorted into different classifications, such as groups with and without contaminants/impurities (e.g., ferrous impurities, non-ferrous impurities like copper and magnesium, and non-metals like plastics and glasses), groups of wrought and cast alloys, and groups of specific alloy series such as 1xxx series to 7xxx series for wrought aluminium. The quality (e. g., purity and specification) of sorted aluminium scraps directly affects their potential for the secondary production of high-quality products (Raabe et al., 2022). Therefore, those high-quality scraps at an alloy level (e.g., groups of wrought and cast alloys, specific alloy series such as 1xxx series to 7xxx series for wrought aluminium) are desired for realising a high-level recycling process. To achieve such alloy-level scrap sorting for enabling high-level recycling towards circular aluminium, an essential step is to develop advanced scrap sorting technologies (Aluminium, 2019), which is the target of this work to be presented in later sections.

In the past decades, various scrap sorting technologies have been developed, such as magnetic separation (e.g., Oberteuffer, 1974), eddy current separation (e.g., Lungu and Rem, 2003), and dense media separation (e.g., Nijhof and Rem, 1999; Coates and Rahimifard, 2009). To meet more complex sorting goals, the current trend of scrap sorting relies on sensors (e.g., visual sensors (Huang et al., 2010), X-ray transmission (XRT) (Mesina et al., 2007), X-ray fluorescence (XRF) (Kölking et al., 2024), and laser-induced breakdown spectroscopy (LIBS) (Hahn and Omenetto, 2012; Park et al., 2021)), artificial intelligence (AI) (Díaz-Romero et al., 2022; Lu and Chen, 2022; Díaz-Romero et al., 2023; Van den Eynde et al., 2023; Xu et al., 2023), and automation (Satav et al., 2023; Kiyokawa et al., 2024). These technologies are being investigated for the high-precision classification of scraps. For example, advanced sensor systems like LIBS (e.g., Hahn and Omenetto, 2012; Park

E-mail address: y.wu-7@tudelft.nl (Y. Wu).

 $^{^{\}ast}$ Corresponding author.

et al., 2021; Van den Eynde et al., 2023) can identify the specific element composition of individual scraps, thus allowing the classification into well-defined alloy types. However, the current running cost of LIBS in real-time sorting processes can be high. A cost-effective alternative, artificial intelligence (AI) in combination with vision systems (e.g., RGB-3D cameras), has attracted the attention of many researchers (Koyanaka and Kobayashi, 2010; Díaz-Romero et al., 2021; Lu and Chen, 2022). Such AI/vision systems were demonstrated to be effective (sorting accuracy from 90 % to 98 %) in sorting aluminium scraps based on scrap shape properties (e.g., particle width, height, and projected area) (Koyanaka and Kobayashi, 2010; Díaz-Romero et al., 2021).

Nevertheless, to achieve a fully operational sorting facility in industrial applications, multiple technologies need to be integrated together, e.g., from scrap feeding, sensor/vision scanning, AI/computer vision, to the robotic picking/ejection of scraps. For feasible and optimal application, it is important to consider the interactions between different technologies/sub-processes in the early design stage. Usually, if the scraps can be fed as a uniform and regular flow on the conveyor belt, the efficiency of subsequent sensor scanning and robotic picking is significantly improved (Pfaff et al., 2016; Rem, 2020; Wen et al., 2021). However, because of the complex shapes of aluminium scraps, many aspects of the scrap flow behaviour are random. For example, scrap pieces can severely overlap on the belt or hook into each other, which impacts the uniform and regular flow, and creates a problem both for effective sensor scanning/computer vision (Lu and Chen, 2022) and for robotic picking of individual scraps. Some devices like vibratory feeders can potentially help to regularize particle flow behaviours including reducing the overlapping of scraps, thus it is critical to have a fundamental understanding of scrap flow dynamics in the processing line which may integrate multiple components (e.g., feeding units like vibratory feeders, conveyor belts, and ejection or picking system) under different operation conditions.

Since scraps are composed of discrete particles, the discrete element method (DEM) (Cundall and Strack, 1979), which has been extensively used for the modelling of particulate systems (Zhu et al., 2008), is promising for understanding scrap flow behaviours and aiding the process design and optimisation. Recently, some researchers have used DEM-based approaches to study recycling processes (e.g., Tsunazawa et al., 2018; Li et al., 2021; Wang and Shen, 2022). Regarding sorting processes, Pieper et al. (2016) studied an automated optical belt sorter for the sorting of bulk solids, in which the particle ejection with air valves was described with the help of a MATLAB script utilizing particle movement information obtained with DEM; the effects of operating parameters like particle shape or conveyor belt length on the sorting quality were systematically investigated. Liu et al. (2022) studied the conveyor belt sorting of coated fuel particles by DEM modelling, where the authors systematically explored the effects of various parameters (e. g., particle sphericity, friction coefficient, belt velocity, and feeding rate) on the efficiency of the system.

Compared with earlier work, the current study focuses on large sizes and complex shapes of the considered scrap particles. First, because the shredding of metals into small sizes can be very energy-intensive and costly, it is beneficial if large-sized scraps can be sorted. In this work in collaboration with an industrial partner, the considered aluminium scraps have a maximum dimension of up to 500 mm. Such scrap size is several times larger than those processed in normal practices where the size of aluminium particles might be about 50 mm (Schloemann, 1982; Zhang et al., 1998) and is orders of magnitude larger than the considered particle sizes in the studies of Pieper et al. (2016) and Liu et al. (2022). Second, the shapes of aluminium scraps are much more complex than previously considered spherical, cubical, and/or cylindrical shapes (Pieper et al., 2016; Liu et al., 2022); and the interaction between complex-shaped particles presents phenomena of clustering and entanglement which are unknown for simpler shapes. Such differences in particle properties are reflected in the design and operation of the sorting system. Hence, to achieve efficient sorting of large and complexshaped aluminium scraps, some new and innovative technologies are essential, and they are studied and optimised in this paper.

In this work, an innovative facility for the efficient sorting of aluminium scraps is presented. The facility integrates newly patented technologies/subprocesses including scrap feeding (Rem et al., 2023c, d), sensor scanning (Staal et al., 2020), and automated ejection (Rem et al., 2023b). The analysis and tests of scrap sorting behaviours in the facility are facilitated by a computational model based on DEM. Specifically, this DEM-based model and its simulation conditions are described in Section 2. After that, Section 3 will present parametric studies by the model and the confirmation of the modelled results through their implementation in actual process lines. Finally, a summary of obtained findings is given in Section 4.

2. Material and methods

2.1. Scrap sorting facility

In the past few years, Delft University of Technology and the Dutch company Myne Circular Metals (https://www.myne.eco/) collaborated to develop an innovative facility (Staal et al., 2020; Rem et al., 2023a, d, c, b) for high-speed automated sorting of metal scraps. The facility can sort large-sized scraps, of which the maximum scrap dimension may be as large as 500 mm, into multiple products by their types (e.g., specific metal alloys). As shown in Fig. 1, this sorting facility integrates three key technologies/sub-processes:

- (1) Singulation, in which the vibratory feeder and chute regularize the initially random scrap flow into an individually spaced very narrow and nearly 1-dimensional (1D) file of scraps on the conveyor belt. By definition, successful singulation means that overlapping of scrap particles is avoided and pieces of scraps can be analysed and picked from the conveyor belt one by one; it can thus readily improve the efficiency of the following sensor scanning and ejection processes.
- (2) Sensor scanning, which uses multiple sensors and/or cameras for the scanning of scraps. The obtained signal information will be processed by AI to distinguish the specific alloy or contaminant group of the scanned scrap. Because many previous studies (e.g., Díaz-Romero et al., 2021; Lu and Chen, 2022) discussed similar technologies in previous work, this part will not be the focus of this paper.
- (3) Ejection, which is realized by a series of cross-like ejectors that are controlled by an automatic system with input information given from prior sensor scanning and the product quality control system. Each of the cross-ejectors corresponds to a well-defined product definition, and the number of ejectors can be set explicitly to match the number of defined scrap types, to meet diverse sorting demands. Such an ejection system owns the potential merit of achieving fast and accurate ejection, while being cost-effective compared with robotic pickers.

2.2. Discrete element method

To aid the understanding and optimization of the scrap flow and the sorting process in the facility as conceptualized in Fig. 1, a virtual experiment-model is developed by DEM, based on the open-source program LIGGGHTS (CFDEM®project; Kloss et al., 2012). In principle, DEM traces both the translational and rotational movement of individual particles according to Newton's second law of motion (Cundall and Strack, 1979). The corresponding governing equations are expressed as:

$$m_i \frac{d\mathbf{v}_i}{dt} = \sum_j (\mathbf{F}_{n,ij} + \mathbf{F}_{t,ij}) + \sum_w (\mathbf{F}_{n,iw} + \mathbf{F}_{t,iw}) + m_i \mathbf{g}$$
 (1)

and

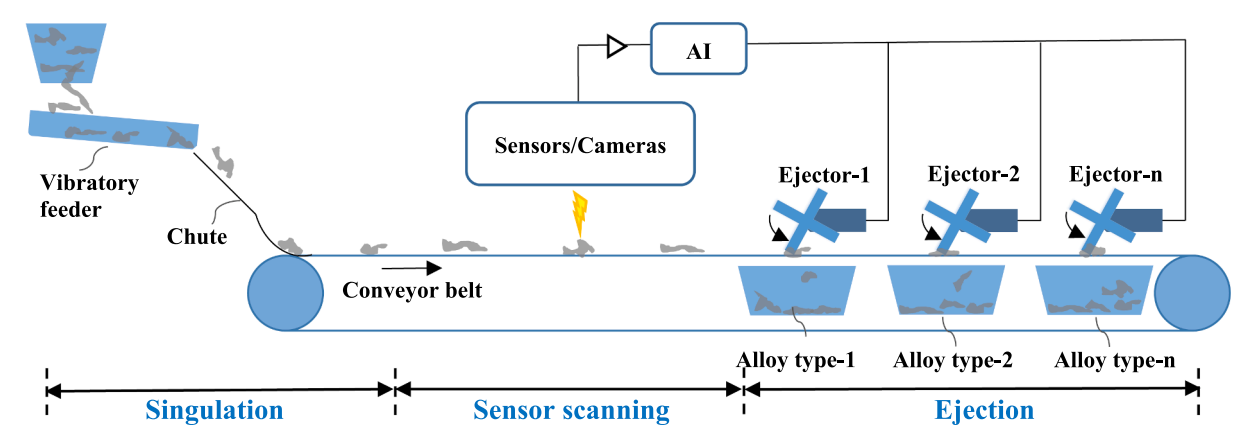


Fig. 1. Conceptual design of the innovative scrap sorting facility.

$$I_{i}\frac{d\omega_{i}}{dt} = \sum_{j} \left(\mathbf{T}_{t,ij} + \mathbf{T}_{r,ij}\right) + \sum_{w} \left(\mathbf{T}_{t,iw} + \mathbf{T}_{r,iw}\right)$$
(2)

where m_i , \mathbf{v}_i , $\mathbf{\omega}_i$ and I_i are the mass, translational and rotational velocities, and the moment of inertia of particle i. The contact forces between particles are calculated based on the Hertz model that considers the normal force $\mathbf{F}_{n,ij}$ and tangential force $\mathbf{F}_{t,ij}$, each of which incorporates both an elastic force term and a damping force term. The torques acting on particle i due to particle j include two components: $T_{t,ij}$ which is generated by the tangential force and $T_{r,ij}$ which is known as the rolling friction torque that is calculated by the constant directional torque (CDT) model in this study. Besides particle-particle interactions, a particle i can also interact with the surfaces or walls of various equipment in the sorting line. In the DEM model, a wall (mesh) element w is considered as a sphere with an infinite radius, thus the particle-wall forces $(\mathbf{F}_{n,iw}, \mathbf{F}_{t,iw})$ and torques $(\mathbf{T}_{t,iw}, \mathbf{T}_{r,iw})$ are computed in a similar manner as particle-particle forces and torques. The detailed equations for computing the force and torque terms can be found in the LIGGGHTS (R)-PUBLIC Documentation (CFDEM®project).

It should be noted that Equations (1) and (2) are only the basic equations of motion and are strictly valid only for spheres; to consider the scrap particles with irregular shapes, two more important

computational models/descriptions are needed. First, the irregular shape of the particle needs to be described properly, using methods like the superellipsoids, discrete function representation, and multisphere method, as described in previous reviews (e.g., Lu et al., 2015; Zhong et al., 2016). In this study, the multisphere model (Kruggel-Emden et al., 2008) is adopted to represent the complex shapes of scrap particles. The forces and torques in the above equations (1-2) are thus the sums of the forces and torques resulting from the element-spheres of scrap particle *i* and particle *j*; for the normal force of the element-sphere that does not pass through the centre of the particle, additional torque is added to Equation (2), which is the cross product of this normal force and the position vector between the element-sphere and the centroid of the particle, of which the expression can be found in previous papers, e.g., Wu et al. (2017). Second, in addition to the overall space-fixed coordinate system, another body-fixed coordinate system (of which the three axes are aligned with the three principal axes of the particle) needs to be used to represent the orientation of each irregular particle. More details regarding the motion and force calculation for non-spherical particles in DEM can be found in previous papers (e.g., Dong et al., 2015; Lu et al., 2015; Zhong et al., 2016).

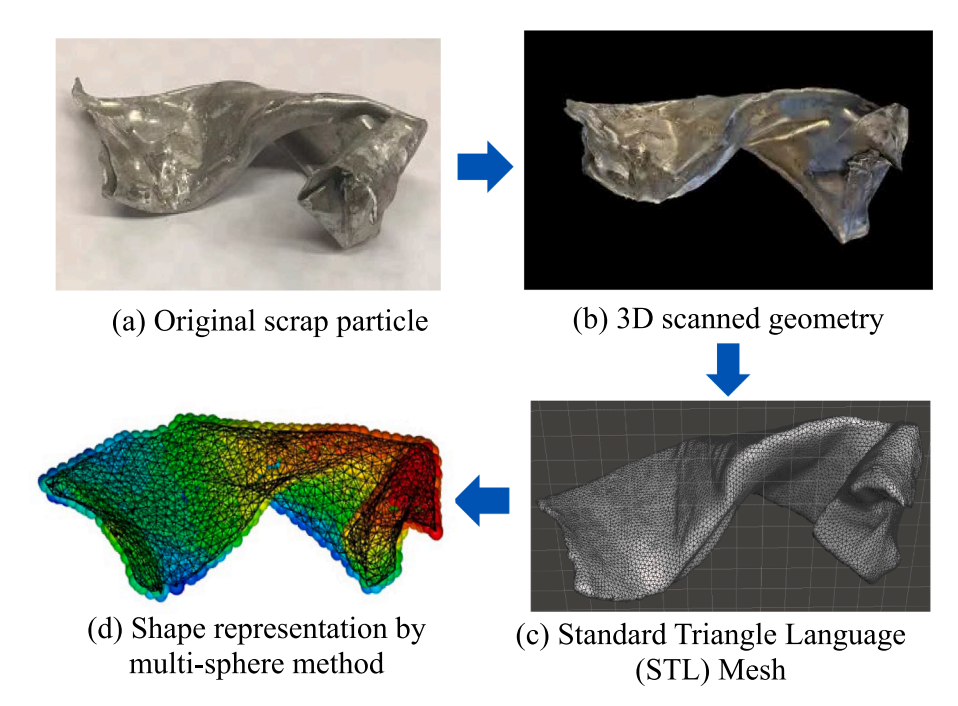


Fig. 2. Shape representation by 3D scanning and multi-sphere method.

2.3. Scrap shape representation

The complex shapes of scraps are described through a procedure as shown in Fig. 2. The realistic 3D geometry of a scrap is scanned and converted to an STL file, based on which the multisphere method (Kruggel-Emden et al., 2008) is used to represent the scrap shape by a series of element (or glued) spheres. Considering the complexity of the scrap shapes, the scraps in the current study are constructed by placing the spheres on the vertices of the STL meshes. This is different from some previous algorithms (Lu and McDowell, 2006), in which the spheres are normally inserted inside the 3D hull of the STL boundary. The reason is that the shapes of considered scraps may contain sharp and thin edges which are more suitable to be represented by a slice of spheres, as shown in Fig. 2(d) The fine meshes of STL are adopted for reaching a better shape accuracy, thus allowing the mass distribution of the constructed/ simulated particle to resemble that of the real particle. Due to the fine meshes, the size of the used element-spheres is selected to be relatively small (e.g., 10 to 20 mm) compared with the dimensions of scrap particles, and a large number of spheres (ranging from 249 to 1699, see Table A.1) is used to describe the scrap shape. Because those elementspheres are overlapped in a scrap particle, the mass density of element-spheres is set to a proper value to guarantee that the overall mass of the constructed scrap particle always matches the actual mass of the real particle, as introduced in a previous study (Lu and McDowell, 2006).

2.4. Automated operation in DEM

The flow chart for computing the automated operation is given in Fig. 3. At every timestep of DEM computation, each scrap particle which has not passed the scanner yet is checked if its position reaches the sensor scanning point and whether it is overlapping with other scraps. If the scrap in the scanning region is overlapping with others, the following sorting steps will not be conducted and it will go to the rest of

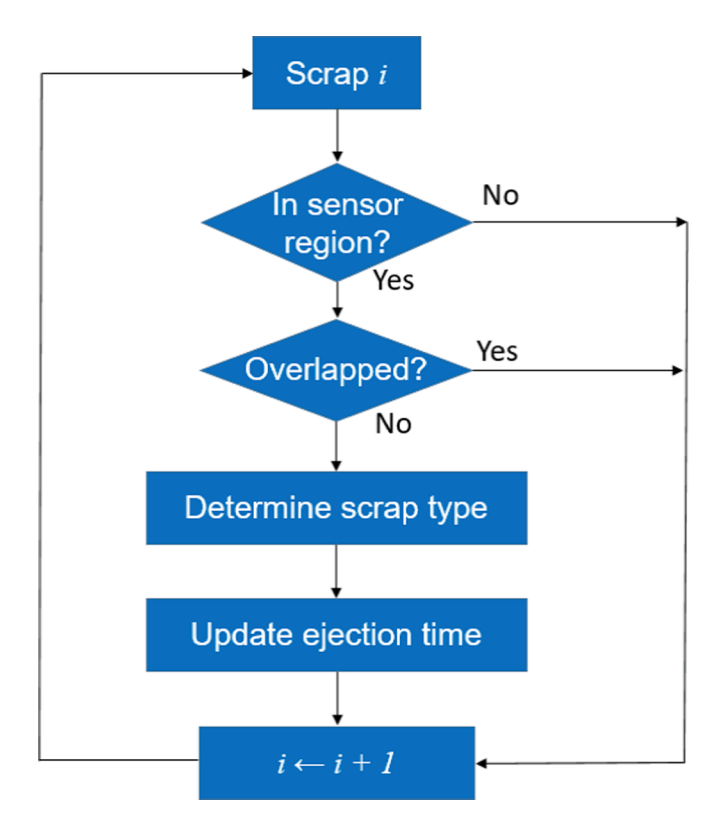


Fig. 3. Flow chart for sensor scanning and automated ejection of scraps at each time step in DEM modelling.

the line. If the scrap does not overlap with other scraps, the type of scrap is determined, and the triggering time of ejection is computed and stored into the ejection time of the specific ejector. Then, if the current timestep is within the ejection timesteps (starting from the time step at triggering to the time step at which an ejection ends) of the ejector, the mesh of the ejector will be rotated; this will lead to the particle ejection by computing the mesh-particle (or particle–wall) force that is available in LIGGGHTS.

2.5. Simulation conditions

For each simulation case, 50 scraps are fed to the system according to a specified feeding rate. Because the current sorting process is a stable process (namely the number of particles in and out of the line is balanced) when the feeding rate of scraps is fixed as a constant, a further increase of the scrap number does not bring an obvious difference in results. The scraps used for simulations are described in Appendix A. In general, five scraps of different shapes and masses are selected from the real scraps, and they are repeatedly and randomly fed into the sorting line according to a specified feed composition and at a specified overall particle feeding rate.

The material parameters of scraps and setups used in the simulations are identified through calibration using experimental data, which is described in Appendix B. Besides, some default values of operation parameters are used in the simulations: the default feeding rate of scraps is 3 per second; the default frequency and amplitude of the vibratory feeder are 40 Hz and 1.4 mm, which are kept constant in this work; and the default speed of the conveyor belt is $3\ m/s$.

3. Results and discussion

3.1. Simulated sorting process

Based on the model developed in Section 2, the virtual experimentmodelling of the whole scrap sorting process is realized, as shown in Fig. 4. At first, different types of scraps are randomly generated and dropped on the vibratory feeder. With the frequency-controlled drives, the vibratory feeder can gently move particles forward, which creates some interparticle space among particles and transports them to the chute at a relatively uniform speed, namely, most particles have a similar speed of around 0.3 m/s before entering the chute. Then, because the chute creates a high acceleration of scrap velocity and makes the flow transition from a wide and nearly 2D flow in the vibratory feeder to a narrow and nearly 1D flow on the conveyor belt, the interparticle distance among particles is realised before the scraps arrive on the conveyor belt. Subsequently, each scrap passes through a sensor region on the conveyor belt, where the type of material is distinguished with the signal information (including type and ejection time) sent to the specific ejector (according to the algorithm described in Section 2.4). Finally, the particles are automatically ejected into the receiving containers by their types, once they reach the ejection points; a video is given in the supplementary material to show this dynamic process.

Even though most scraps are sorted in one go, there can still be scraps that are in clustering with each other (not singulated) and they will go to the end of the line (e.g., the end container in Fig. 4). For treating such unsorted scraps, there can be multiple options, such as sorting in another iteration of the processing line, or sorting in another subsequent processing line that applies different facilities, or directly selling them as products. The selection of such options may depend on the added value after processing the unsorted materials and the operational cost of the iterative/subsequent processing line. For this study, the primary focus is on optimising the proposed sorting facility so that the most scraps can be sorted in one go. The iterative processing of unsorted materials or the processing of the rest with some subsequent facilities may be studied in future.

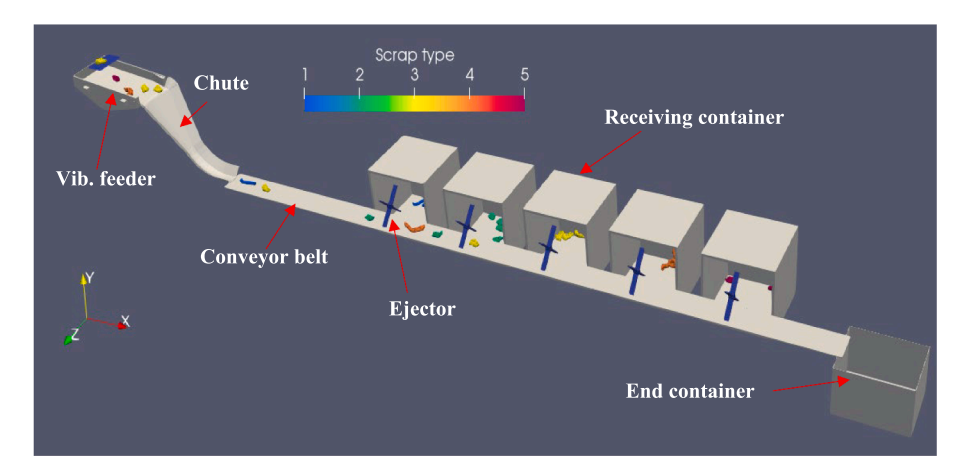


Fig. 4. The equipment and sorting process in the DEM simulation.

3.2. Effect of feeding rate

The scrap flow and sorting behaviour are affected by various parameters. Among them, the feeding rate (defined as the number of scrap particles fed per second) is the most influential parameter. In practice, if a larger amount of materials is fed into the processing line at a certain time, then a higher feeding rate (i.e., a higher number of particles per second) will be created. On the one hand, the feeding rate can influence the throughput of the production, i.e., a higher feeding rate corresponds to a larger amount of processed materials. On the other hand, the feeding rate can also influence the sorting rate that is defined as the percentage of sorted particles among all the particles fed into the line. The successful sorting of a particle requires the singulation of the particle with a certain interparticle distance (e.g., larger than 0.05 m for this work) between the considered particle and its neighbouring particles (e. g., the one before or after it), as a condition for the subsequent successful/accurate sensor scanning and ejection. Hence, a higher feeding rate can lead to a very dense flow of particles (with possibly reduced interparticle distance) and corresponding more clusters as failed sorting particles. Therefore, it is important to understand the influence of feeding rate, for identifying a suitable parameter for optimal production.

In Fig. 5(a-c), the simulated scrap flows at different feeding rates are visualized (while the belt speed is kept at 3 m/s). At a low feeding rate (e. g., $N_s = 1$ /s), the arrived scrap flow on the conveyor belt is diluted with large interparticle space. With the increase of feeding rate (e.g., $N_s = 3$ /s), the flow becomes denser with a decreased average interparticle space. At a high feeding rate (e.g., $N_s = 5$ /s), scraps are likely to be very close or even overlapping with their neighbours, resulting in clusters that cannot be separated by the ejectors. Hence, the sorting rate generally decreases with the increase of feeding rate, which is also quantitatively shown in Fig. 5(d). From the view of optimization, the target is to reach both a high sorting rate for avoiding too many particles unsorted and a high throughput (corresponding to many particles sorted per second) for economic reasons. In Fig. 5(d), it is noted that there is a relatively slower decrease of sorting rate when N_s is increased from 2 /s to 4/s, which indicates $N_s = 3$ or 4/s should be the suitable feeding rate to allow a relatively high throughput while maintaining a high sorting rate.

3.3. Effect of belt speed

The belt speed is another critical factor in affecting the singulation and sorting rates. Because the successful sorting of a particle requires certain interparticle space between the particle and its neighbouring particles (the one prior or behind it) as a condition for the subsequent successful ejection. Here, the effect of the variation of the belt speed (V_{belt}) from 2.0 m/s to 4.0 m/s on the sorting rate (while the feeding rate

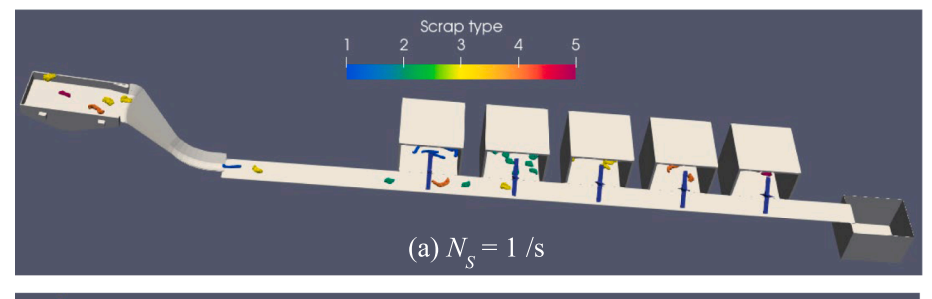
is kept at 3 /s) is investigated. As shown in Fig. 6, the sorting rate increases obviously with the increase of V_{belt} . The underlying reasons can be understood from the scrap flow behaviour at the chute-to-belt transition. The mean velocity of scrap particles exiting the chute (V_{chute_exit}) is about 2.96 m/s (Table C.3), thus the scraps will experience either deceleration or acceleration at the chute-to-belt transition, depending on whether V_{belt} is lower or higher than V_{chute_exit} . Accordingly, the deceleration of scraps in the transition leads to a decrease of interparticle distance between scraps (Fig. 6 (b) and (c)) and thus decreases the sorting rate. By comparison, the acceleration of scraps will increase the interparticle distance between scraps, thus some failed singulation cases with no interparticle distance that cannot be sorted (Fig. 6(d)) are transformed into successful singulation cases with desirable interparticle distance for sorting operations (Fig. 6(e)). As a result, this increases the sorting rate of particles.

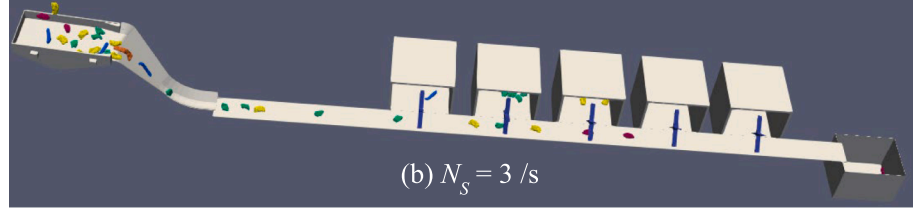
Regarding the overall relationship between V_{belt} and sorting rate (Fig. 6(a)), a high gradient of change is witnessed for V_{belt} decreasing from 3 m/s to 2 m/s (corresponding to the phase with $V_{belt} < V_{chute_exit}$), implying that the decrease of V_{belt} below V_{chute_exit} will result in a quick drop of the sorting rate. On the other hand, from the view of industrial implementation, although the increase of V_{belt} can improve the singulation of particles, a high V_{belt} will also require a faster speed of sensor scanning, AI computation, and automatic scrap ejection. In other words, the increase of V_{belt} should be considered together with the processing capability of other equipment as well, which might be a relevant limitation in real applications. For the facility considered in this study, $V_{belt} \geq 3$ m/s is used (with $V_{belt} = 3$ m/s as the default value).

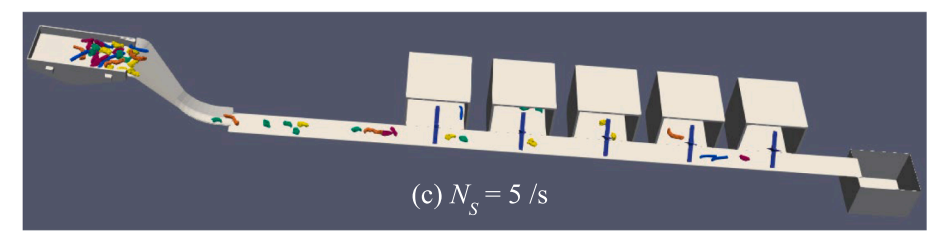
3.4. Effect of scrap shape

It is known that particle shape can have important effects on the flow behaviours of particulate systems (Dong et al., 2015; Lu et al., 2015; Zhong et al., 2016). As described in Section 2.3 and Appendix A, the simulations considered five scrap types; these types were fed to the simulation cases of previous sections according to a default composition ratio. Here, to consider the effect of scrap shape, the composition ratio was varied for the five scrap types that have aspect rations from 1.69 to 5.56 and scrap length from 0.199 to 0.416 m (see Appendix A for details), thus creating a series of simulation cases with varying mean aspect ratio ($\langle AR \rangle$) and mean scrap length ($\langle L \rangle$), at a constant feeding rate N=3/s and a constant belt speed at 3 m/s.

Two typical cases of scrap flows with different shapes are compared in Appendix C. It is shown that scraps with larger aspect ratios and longer lengths will have preferential orientation along the flow direction when they flow down in the chute and are more difficult to rearrange their positions in the chute, which can result in more clustered or parallel scrap pairs on the belt, thus deteriorating the sorting efficiency.







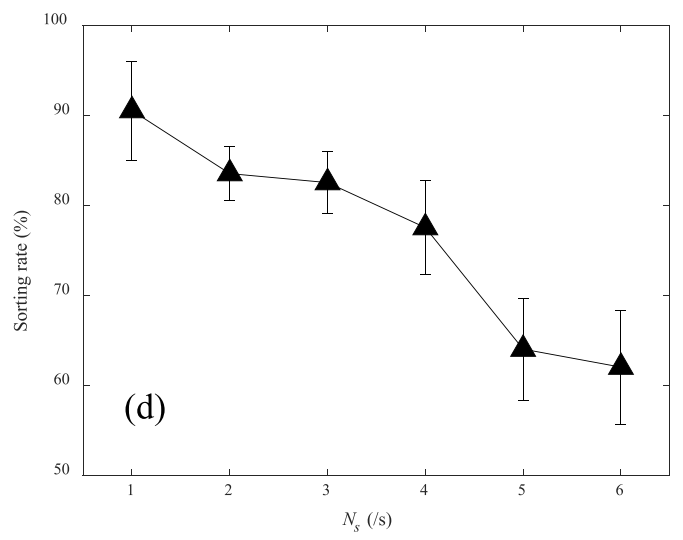


Fig. 5. Effects of different feeding rates (N_s) .

More quantitative results of the sorting rates with varying < AR>and < L>are given in Fig. 7. The general trend is that the sorting rate tends to decrease continually with the increase of < AR>or < L>. At a large < AR> (e.g., > 3.2) or a large < L> (e.g., > 0.32 m), the resulting sorting rates of individual simulations are also strongly fluctuating, with a large standard deviation of the value as indicated in the error bar (the last points of Fig. 7 (a) and (b)). This indicates that the scrap sorting process at those large < AR>or large < L>conditions may not be stable and controllable. Besides, on the other hand, from the scatter plot in Fig. 7 (c), a high sorting rate is normally obtained at both a small < AR>and a small < L>, and vice versa.

Overall, the results in this section indicate the important effects of scrap shape on the flow and the sorting behaviour. Because the sorting of scraps with a small < AR>and a small < L>can be more efficient, it should be very beneficial to achieve a higher sorting rate by feeding scraps with a small < AR>and a small < L>, which may be realized in suitable shredding and screening processes prior to the feeding into the

sorting line.

It is noted that the results and discussion here are based on a constant feeding rate of $N_S=3$ /s. In reality, the overall sorting efficiency or processing capability of a sorting line may be more often evaluated by the mass of scraps (instead of the number of scraps) being successfully sorted in a certain time. Then, for the shredding process to improve the shape (for a small $\langle AR \rangle$ and a small $\langle L \rangle$), there can be two possible results: (1) improved particle shape while keeping similar average particle mass, by ideally just making those particles of large AR and/or L more twisted and compacted (specific equipment/technology for achieving such results may be explored in future work); (2) improved scrap shape while increasing the number of resultant particles and reducing the average particle mass, by possibly breaking those particles with large AR and/or large L into more particles of smaller size. Generally, the first result is more desirable and may be realized by the well-designed shredder equipment and/or suitable shredding operation. For the second result, some of those smaller-sized particles should be

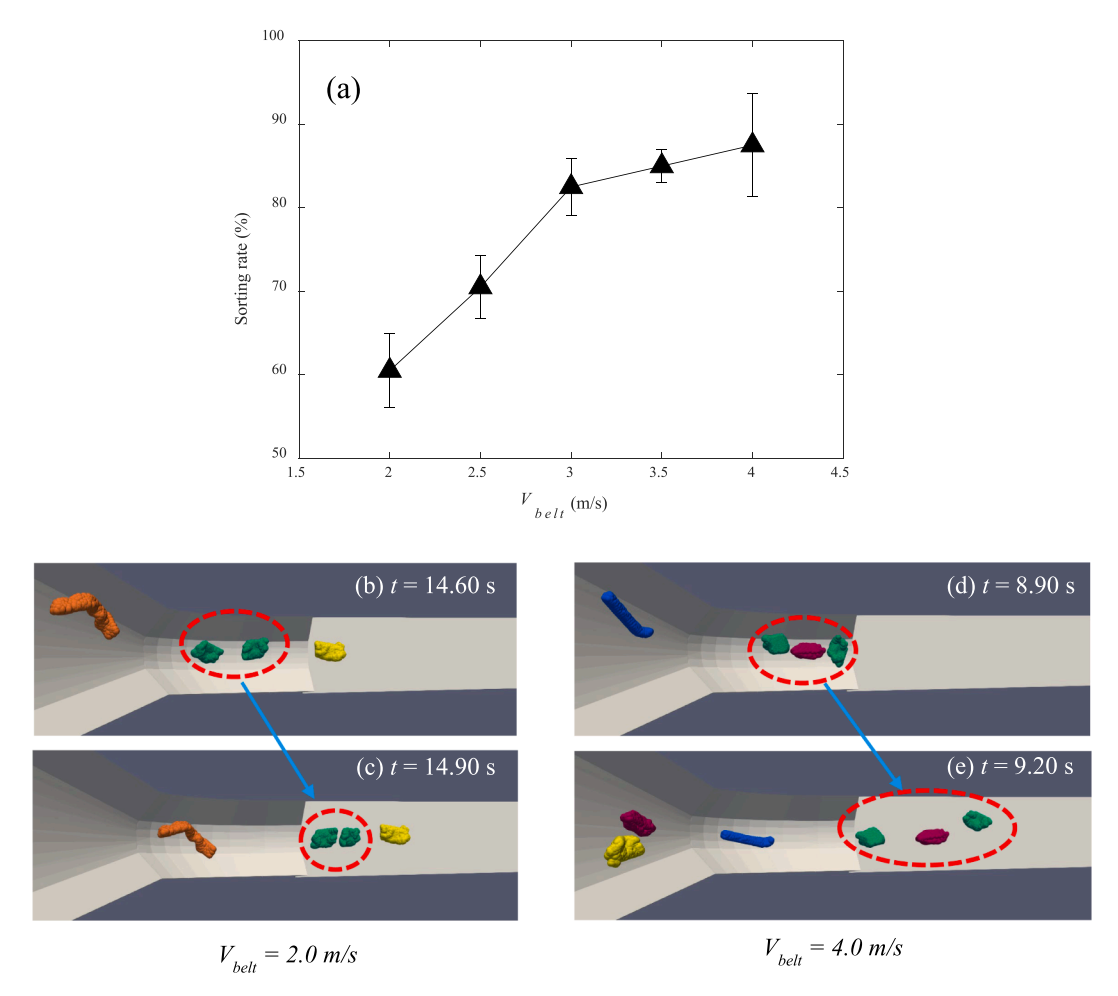


Fig. 6. Effects of different belt speeds (V_{belt}).

screened into another particle fraction which will be fed at an increased feeding rate into the processing line, thus keeping a similar mass processing rate as well.

3.5. Implementation in actual processing lines

The design and proposed results from DEM modelling were tested and implemented at Myne Circular Metals, as shown in Fig. 8. At similar settings as in the simulations (e.g., feeding rate of 3/s and belt speed of 3 m/s), the actual tests (e.g., Fig. 8(a)) reached a singulation rate (defined as the percentage of singulated particles with desired interparticle distance (e.g., > 0.05 m for this case) among all the particles that are fed into the processing line) of about 83 % (from 78 % to 85 %). Such tested results thus confirmed the simulated results, e.g., a simulated sorting rate about 80 % in Fig. 5; note that the singulation rate is comparable to the sorting rate in this study, as every singulated scrap is also successfully sorted. The automated ejection of scraps has also been realized to quickly sort scraps into product bins (e.g., up to 5–7 scraps per second). On such a basis, a full plant named "Xorter" (Fig. 8 (c)) has been built with 8 processing lines and 8 robotic ejectors for each line (64 robotics running at the same time), enabling the sorting of scraps into diverse metal alloys according to the demands of customers (e.g., various smelters and manufacturers).

3.6. Discussion

The obtained results show that the proposed innovative scrap sorting facility is feasible for realizing a well-singulated flow of scraps and sorting scraps automatically and efficiently at a fast speed (e.g., 3–4

scraps per second for a sorting rate of about 83 %). By means of a virtual experiment, DEM simulation has optimized the design and operation of the facility and demonstrated with experimental tests that this type of facility can bring:

- (1) High efficiency: considering the scraps are relatively large in size (max. dimension up to 500 mm which is much larger than the normal scrap size around 50 mm (Schloemann, 1982)), the sorted efficiency of scraps in terms of weight/mass can be desirable. For instance, at a feeding rate of 3 scraps per second with a sorting rate of about 80 % and considering the mean scrap weight of around 0.25 kg, the output can reach around 2.2 t/h for one processing line, which is promising for commercialisation in industrial applications.
- (2) Flexibility: the facility is flexible in sorting a variable number of scrap types and a variable amount of the overall production target. First, for each sorting facility, the number of ejectors can be flexibly changed to sort a variable number of products defined by the users; the product number can be very large (e.g., > 10), as long as the sensor/AI system can sustain the processing load. Second, an industrial plant may parallelly combine several such sorting facilities/lines, thus achieving the high production target desired by users.

Compared with some existing technologies/facilities of sorting objects/scraps on 2D conveyor belt (Brooks et al., 2019; Engelen et al., 2022; Satav et al., 2023), the proposed sorting facility/technology is featured in its capability to realise nearly 1D flow of scraps (see Figs. 4, 5 and 8). In the transition from the sorting of a 2D flow to the current

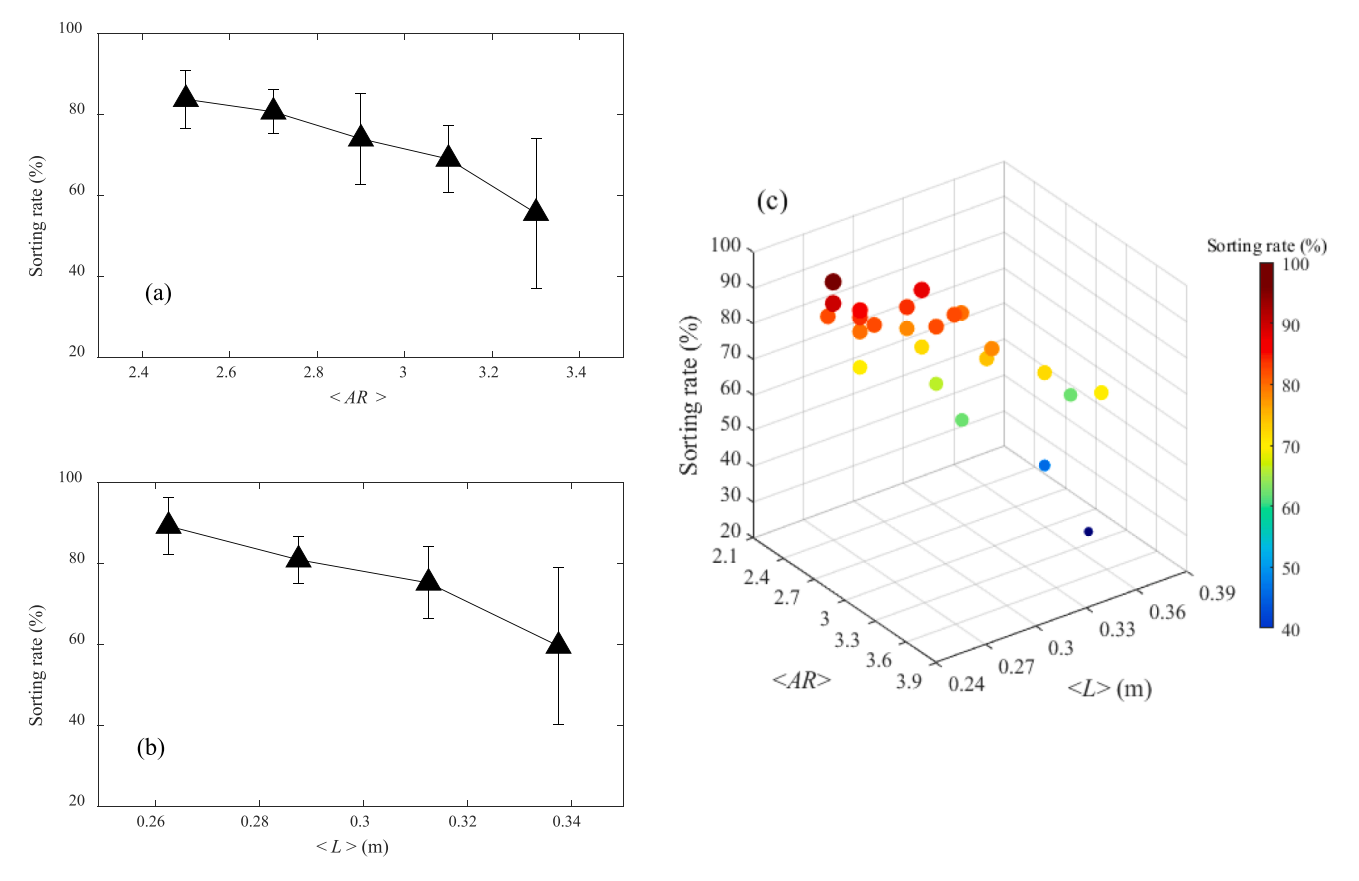


Fig. 7. Sorting rate vs. scrap shape parameters: (a) Sorting rate vs. mean aspect ratio (<AR>); (b) Sorting rate vs. mean scrap length (<L>); (c) Sorting rate vs. the combined effect of mean aspect ratio (<AR>) and mean scrap length (<L>) at a constant feeding rate N $_s = 3$ /s.

sorting of several 1D flows, there are extra costs but also added benefits. The extra costs come from the multiplication of lines (e.g., feeding units, conveyors, sensors, and ejectors), while the added benefits come from the desired high number of products sorted by a series of ejectors. Besides, as scrap ejection is less sensitive to scrap properties (e.g., shape and weight) compared with robotic picking (Satav et al., 2023), the ejection system can be robust and accurate in sorting scraps that have diverse properties, e.g., various shapes, surfaces, and weight. As such, the current system is being implemented in the industry.

Other than the sorting facility, this work conducted virtual experiment-modelling by DEM to understand the details of the scrap sorting behaviours. Especially, it is found that the singulation process which regularizes the flow behaviour of scraps with proper interparticle distance is crucial for a successful sorting operation. Based on parametric studies, solutions are proposed for the optimal operation of the singulation process. The concept and the obtained insights in this study should be very useful for transferring those AI techniques, which generally assume the waste scraps are put on the conveyor belt one by one (Lu and Chen, 2022), into real industrial applications.

However, it should also be noted that there are some limitations in this work which require further studies in future. First, only five types of scrap shapes have been considered; for a deeper understanding of the shape effect, more shape properties (e.g., area, volume, and curvature) may be considered together by some statistical or data-driven models. Second, while the current work is mainly focused on the scrap flow behaviours under various operational conditions, the effect and optimization of equipment geometry (e.g., vibratory feeder, chute, and ejector) are also worthy of further study. Third, a more quantitative understanding of the scrap flow dynamics, such as the mathematical description of the delay time series of scraps' arrival on the belt and the more reasonable description of the rolling/sliding and damping/rebounding dynamics (Beunder and Rem, 2003) of such non-round/

complex-shaped particles, may also be further explored in future. In addition, the DEM-based models as described in this study are mainly used for offline process design and optimisation nowadays, due to their high computational cost. It will be interesting for future studies to improve the computational speed of such DEM-based models (by potentially combining DEM with some data-driven or machine learning methods), thus realising the online process control and optimization.

4. Conclusions

An innovative sorting facility for the automated sorting of aluminium scraps has been presented in this study. The facility is aimed at sorting a mixed scrap flow at an individual particle level, thus classifying scraps into multiple products of specified alloy types (e.g., wrought and cast alloys, specific alloy series such as 1xxx series to 7xxx series for wrought aluminium). The sorting process is computationally studied by a virtual experiment model developed from DEM. Based on parametric studies of some key design and operational factors as well as particle properties, insights are obtained for better process design and optimization. The main findings are summarized as follows.

(1) It is feasible to integrate the automated singulation of scrap flow, sensor scanning, and ejection into a highly efficient sorting facility. In particular, based on a proper design and operation of the feeding setup, the singulation of scraps is achieved and results in an individually spaced very narrow and nearly 1D file of scraps on the conveyor belt, being a great basis for the following effective sensor scanning and scrap ejection. Besides, the accurate ejection of different types of scraps by a series of cross-like ejectors is also shown to be feasible, thus offering an accurate, fast, and cost-effective way for automated sorting of scraps.

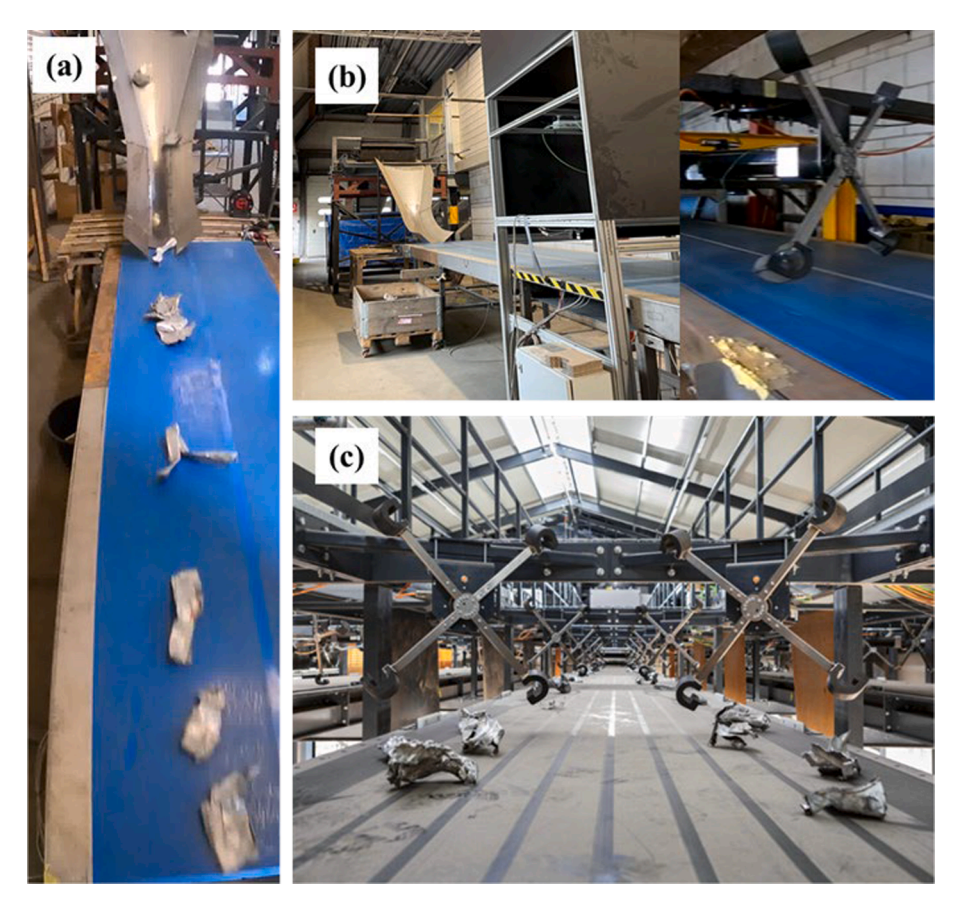


Fig. 8. The implementation of the design and results at Myne Circular Metals: (a) singulation prototype; (b) pilot-scale test line; (c) full-scale plant.

- (2) Both operational parameters and scrap shapes have important influences on the scrap flow and sorting behaviours. In particular, the increase of feeding rate leads to an increasingly denser flow in the setup, thus deteriorating the sorting rate; the feasible range of feeding rate in this application (for particle size up to 500 mm) may be around 3-4 particles per second which can realize a sorting rate of around 83 % (as a compromise to reach both a high sorting rate for avoiding too many particles unsorted and a high throughput for economic reasons), and the sorting rate will drop quickly for feeding rate beyond 5 particles per second. Besides, suitable scrap shapes are from equal-sided to relatively elongated shapes, with an aspect ratio from 1 to 3. Those infeed scrap batches with larger mean aspect ratios (e.g., > 3.2) and longer mean lengths (e.g., > 0.32 m) can result in more clustered or parallel scrap pairs on the belt, thus reducing the sorting efficiency.
- (3) A computational model for modelling the scrap sorting process is developed in this work, based on the particle-scale DEM. Besides the consideration of realistic scrap shapes and the computation at a full scale of the pilot-scale processing line, the fascinating merit of the model is it has successfully integrated sensor scanning and automated ejection with the particle flow dynamics, thus allowing it to be a virtual experiment model. As in our current project with industrial partner Myne Circular Metals, such a model has been used for obtaining useful insights into complex scrap flow phenomena and aiding in a cost-effective process design and optimization.

At last, it should be noted that although this study is mainly focused on the sorting of aluminium scraps, the introduced facility and technologies can also be potentially applied to the sorting of many other products, including various metal scraps (e.g., steel, copper), composite

materials, and electronic wastes. It may also be able to sort several different materials at once as long as the flow behaviours of materials are well regularized in the processing line, while this is subjected to future study.

CRediT authorship contribution statement

Yongli Wu: Writing – original draft, Visualization, Validation, Software, Methodology, Investigation, Funding acquisition, Formal analysis, Data curation, Conceptualization. Tijmen Oudshoorn: Validation, Resources, Investigation, Formal analysis, Data curation. Peter Rem: Writing – review & editing, Supervision, Resources, Project administration, Methodology, Investigation, Funding acquisition, Formal analysis, Conceptualization.

Declaration of competing interest

The authors declare the following financial interests/personal relationships which may be considered as potential competing interests: [Yongli Wu has patent Recycling of scrap issued to Technische Universiteit Delft. Peter Rem has patent Recycling of scrap issued to Technische Universiteit Delft. Tijmen Oudshoorn is currently employed at Myne Circular Metals. If there are other authors, they declare that they have no known competing financial interests or personal relationships that could have appeared to influence the work reported in this paper].

Data availability

The authors are unable or have chosen not to specify which data has been used.

Acknowledgement

The authors would like to acknowledge the financial support from Dutch company Myne Circular Metals (formerly Reukema) and EU Horizon Marie Skłodowska-Curie Project (SortCAS, No. 101066062). Besides, this work made use of the Dutch national e-infrastructure with the support of the SURF Cooperative using grant no. EINF-3045, which is also acknowledged.

Appendix A. Supplementary material

Supplementary data to this article can be found online at https://doi.org/10.1016/j.wasman.2024.08.018.

References

- Aluminium, E., 2019. Vision 2050: European aluminium's contribution to the EU's midcentury low-carbon roadmap. Belgium, Brussels.
- Beunder, E.M., Rem, P.C., 2003. The motion of a rolling polygon. J. Appl. Mech. 70 (2), 275–280. https://doi.org/10.1115/1.1481893.
- Brooks, L., Gaustad, G., Gesing, A., Mortvedt, T., Freire, F., 2019. Ferrous and non-ferrous recycling: challenges and potential technology solutions. Waste Manag. 85, 519–528. https://doi.org/10.1016/j.wasman.2018.12.043.
- $\label{lem:complex} CFDEM@roject, CFDEM@coupling Documentation, Version 3.X. \ https://www.cfdem.com/media/CFDEM/docu/CFDEMcoupling_Manual.html.$
- Coates, G., Rahimifard, S., 2009. Modelling of post-fragmentation waste stream processing within UK shredder facilities. Waste Manag. 29 (1), 44–53. https://doi. org/10.1016/j.wasman.2008.03.006.
- Cundall, P.A., Strack, O.D.L., 1979. A discrete numerical model for granular assemblies. Géotechnique 29 (1), 47–65. https://doi.org/10.1680/geot.1979.29.1.47.
- Díaz-Romero, D., Sterkens, W., Van den Eynde, S., Goedemé, T., Dewulf, W., Peeters, J., 2021. Deep learning computer vision for the separation of cast- and wroughtaluminum scrap. Resour. Conserv. Recycl. 172, 105685 https://doi.org/10.1016/j. resconrec.2021.105685.
- Díaz-Romero, D.J., Van den Eynde, S., Sterkens, W., Engelen, B., Zaplana, I., Dewulf, W., Goedemé, T., Peeters, J., 2022. Simultaneous mass estimation and class classification of scrap metals using deep learning. Resour. Conserv. Recycl. 181 https://doi.org/ 10.1016/j.rescorrec.2022.106272.
- Díaz-Romero, D., Van den Eynde, S., Zaplana, I., Zhou, C., Sterkens, W., Goedemé, T., Peeters, J., 2023. Classification of aluminum scrap by laser induced breakdown spectroscopy (LIBS) and RGB + D image fusion using deep learning approaches. Resour. Conserv. Recycl. 190 https://doi.org/10.1016/j.resconrec.2023.106865.
- Dong, K., Wang, C., Yu, A., 2015. A novel method based on orientation discretization for discrete element modeling of non-spherical particles. Chem. Eng. Sci. 126, 500–516. https://doi.org/10.1016/j.ces.2014.12.059.
- Engelen, B., Marelle, D.D., Diaz-Romero, D.J., den Eynde, S.V., Zaplana, I., Peeters, J.R., Kellens, K., 2022. Techno-economic assessment of robotic sorting of aluminium scrap. Procedia CIRP 105, 152–157. https://doi.org/10.1016/j.procir.2022.02.026.
- Hahn, D.W., Omenetto, N., 2012. Laser-induced breakdown spectroscopy (LIBS), part II: review of instrumental and methodological approaches to material analysis and applications to different fields. Appl. Spectrosc. 66 (4), 347–419. https://doi.org/ 10.1366/11-06574.
- Huang, J., Pretz, T., Bian, Z., 2010. Intelligent solid waste processing using optical sensor based sorting technology, 2010 3rd International Congress on Image and Signal Processing. pp. 1657-1661.
- Kiyokawa, T., Takamatsu, J., Koyanaka, S., 2024. Challenges for future robotic sorters of mixed industrial waste: a survey. IEEE Trans. Autom. Sci. Eng. 21 (1), 1023–1040. https://doi.org/10.1109/tase.2022.3221969.
- Kloss, C., Goniva, C., Hager, A., Amberger, S., Pirker, S., 2012. Models, algorithms and validation for opensource DEM and CFD-DEM. Prog. Comput. Fluid Dyn. 12 (2–3), 140–152.
- Kölking, M., Flamme, S., Heinrichs, S., Schmalbein, N., Jacob, M., 2024. More resource efficient recycling of copper and copper alloys by using X-ray fluorescence sorting systems: An investigation on the metallic fraction of mixed foundry residues. Waste Manage. Res. https://doi.org/10.1177/0734242x241241601, 0734242X241241601.
- Koyanaka, S., Kobayashi, K., 2010. Automatic sorting of lightweight metal scrap by sensing apparent density and three-dimensional shape. Resour. Conserv. Recycl. 54 (9), 571–578. https://doi.org/10.1016/j.resconrec.2009.10.014.
- Kruggel-Emden, H., Rickelt, S., Wirtz, S., Scherer, V., 2008. A study on the validity of the multi-sphere Discrete Element Method. Powder Technol. 188 (2), 153–165. https:// doi.org/10.1016/j.powtec.2008.04.037.
- Li, Y., Qin, X., Zhang, Z., Dong, H., 2021. Operation parameters optimization of a separating system for non-ferrous metal scraps from end-of-life vehicles based on coupled simulation. Waste Manag. 120, 667–674. https://doi.org/10.1016/j. wasman.2020.10.032.
- Liu, Z., Ma, H., Fan, T., Liu, M., Zhao, Y., 2022. DEM investigation of the conveyor belt sorting system for coated fuel particles with a large feeding rate. Powder Technol. 399 https://doi.org/10.1016/j.powtec.2022.117160.

- Lu, W., Chen, J., 2022. Computer vision for solid waste sorting: a critical review of academic research. Waste Manag. 142, 29–43. https://doi.org/10.1016/j. www.n. 2023.02.000
- Lu, M., McDowell, G.R., 2006. The importance of modelling ballast particle shape in the discrete element method. Granul. Matter 9 (1–2), 69–80. https://doi.org/10.1007/ s10035-006-0021-3.
- Lu, G., Third, J.R., Müller, C.R., 2015. Discrete element models for non-spherical particle systems: from theoretical developments to applications. Chem. Eng. Sci. 127, 425–465. https://doi.org/10.1016/j.ces.2014.11.050.
- Lungu, M., Rem, P., 2003. Eddy-current separation of small nonferrous particles by a single-disk separator with permanent magnets. IEEE Trans. Magn. 39 (4), 2062–2067. https://doi.org/10.1109/tmag.2003.812724.
- Mesina, M.B., de Jong, T.P.R., Dalmijn, W.L., 2007. Automatic sorting of scrap metals with a combined electromagnetic and dual energy X-ray transmission sensor. Int. J. Miner. Process. 82 (4), 222–232. https://doi.org/10.1016/j.minpro.2006.10.006.
- Nijhof, G.H., Rem, P.C., 1999. Upgrading of non-ferrous metal scrap, particularly aluminum, for recycling purposes. JOM 1083–1086.
- Oberteuffer, J., 1974. Magnetic separation: a review of principles, devices, and applications. IEEE Trans. Magn. 10 (2), 223–238. https://doi.org/10.1109/ TMAG.1974.1058315.
- Park, S., Lee, J., Kwon, E., Kim, D., Shin, S., Jeong, S., Park, K., 2021. 3D sensing system for laser-induced breakdown spectroscopy-based metal scrap identification. Int. J. Precis. Eng. Manuf. - Green Technol. https://doi.org/10.1007/s40684-021-00364-1.
- Pfaff, F., Pieper, C., Maier, G., Noack, B., Kruggel-Emden, H., Gruna, R., Hanebeck, U.D., Wirtz, S., Scherer, V., Längle, T., Beyerer, J., 2016. Simulation-Based Evaluation of Predictive Tracking for Sorting Bulk Materials. In: 2016 IEEE International Conference on Multisensor Fusion and Integration for Intelligent Systems (MFI), pp. 511–516.
- Pieper, C., Maier, G., Pfaff, F., Kruggel-Emden, H., Wirtz, S., Gruna, R., Noack, B., Scherer, V., Längle, T., Beyerer, J., Hanebeck, U.D., 2016. Numerical modeling of an automated optical belt sorter using the Discrete Element Method. Powder Technol. 301, 805–814. https://doi.org/10.1016/j.powtec.2016.07.018.
- Raabe, D., Ponge, D., Uggowitzer, P.J., Roscher, M., Paolantonio, M., Liu, C., Antrekowitsch, H., Kozeschnik, E., Seidmann, D., Gault, B., De Geuser, F., Deschamps, A., Hutchinson, C., Liu, C., Li, Z., Prangnell, P., Robson, J., Shanthraj, P., Vakili, S., Sinclair, C., Bourgeois, L., Pogatscher, S., 2022. Making sustainable aluminum by recycling scrap: the science of "dirty" alloys. Prog. Mater Sci. 128 https://doi.org/10.1016/j.pmatsci.2022.100947.
- Rem, P.C., Wu, Y., Di Maio, F., 2023a. Recycling of scrap, WO2023224478A1.
 Rem, P.C., Wu, Y., Di Maio, F., 2023b. Recycling of scrap (Scrap selector ejector), NI.2031878B1.
- Rem, P.C., Wu, Y., Di Maio, F., 2023c. Recycling of scrap (Scrap selector infeed), NL2031877B1.
- Rem, P.C., Wu, Y., Di Maio, F., 2023d. Recycling of scrap (Scrap selector process layout), NL2031879B1.
- Rem, P.C., Berkhout, S.P.M., Van Beek, C., 2020. Apparatus and method for picking up objects off a surface. WO2020242298A1.
- Satav, A.G., Kubade, S., Amrutkar, C., Arya, G., Pawar, A., 2023. A state-of-the-art review on robotics in waste sorting: scope and challenges. Int. J. Interact. Design Manuf. (IJIDeM) 17 (6), 2789–2806. https://doi.org/10.1007/s12008-023-01320-w.
- Schloemann, E., 1982. Eddy-current techniques for segregating nonferrous metals from waste. Conserv. Recycl. 5 (2), 149–162. https://doi.org/10.1016/0361-3658(82)
- Soo, V.K., Peeters, J., Paraskevas, D., Compston, P., Doolan, M., Duflou, J.R., 2018. Sustainable aluminium recycling of end-of-life products: a joining techniques perspective. J. Clean. Prod. 178, 119–132. https://doi.org/10.1016/j. jclepro.2017.12.235.
- Staal, H., Van de Poll, M., Berkhout, S.P.M., Rem, P.C., 2020. Process and apparatus for scrap metal scanning, US10830748B2.
- Tsunazawa, Y., Hisatomi, S., Murakami, S., Tokoro, C., 2018. Investigation and evaluation of the detachment of printed circuit boards from waste appliances for effective recycling. Waste Manag. 78, 474–482. https://doi.org/10.1016/j. wasman.2018.06.024.
- Van den Eynde, S., Díaz-Romero, D.J., Zaplana, I., Peeters, J., 2023. Deep learning regression for quantitative LIBS analysis. Spectrochim. Acta B At. Spectrosc. 202 https://doi.org/10.1016/j.sab.2023.106634.
- Van der Voet, E., Van Oers, L., Verboon, M., Kuipers, K., 2018. Environmental implications of future demand scenarios for metals: methodology and application to the case of seven major metals. J. Ind. Ecol. 23 (1), 141–155. https://doi.org/ 10.1111/jiec.12722.
- Wang, S., Shen, Y., 2022. Particle-scale modelling of the pyrolysis of end-of-life solar panel particles in fluidized bed reactors. Resour. Conserv. Recycl. 183 https://doi. org/10.1016/j.resconrec.2022.106378.
- Watari, T., Nansai, K., Nakajima, K., 2021. Major metals demand, supply, and environmental impacts to 2100: a critical review. Resour. Conserv. Recycl. 164, 105107 https://doi.org/10.1016/j.resconrec.2020.105107.
- Wen, P., Lohlefink, G., Rem, P., 2021. Non-overlapping coverage in random feeding. Powder Technol. 385, 50–59. https://doi.org/10.1016/j.powtec.2021.02.068.
- Wu, Y., An, X., Yu, A., 2017. DEM simulation of cubical particle packing under mechanical vibration. Powder Technol. 314, 89–101. https://doi.org/10.1016/j. powtec.2016.09.029.
- Xu, W., Xiao, P., Zhu, L., Zhang, Y., Chang, J., Zhu, R., Xu, Y., 2023. Classification and rating of steel scrap using deep learning. Eng. Appl. Artif. Intel. 123 https://doi.org/ 10.1016/j.engappai.2023.106241.

- Zhang, S., Forssberg, E., Arvidson, B., Moss, W., 1998. Aluminum recovery from electronic scrap by High-Force® eddy-current separators. Resour. Conserv. Recycl. 23 (4), 225–241. https://doi.org/10.1016/S0921-3449(98)00022-6.
 Zhong, W., Yu, A., Liu, X., Tong, Z., Zhang, H., 2016. DEM/CFD-DEM modelling of non-
- Zhong, W., Yu, A., Liu, X., Tong, Z., Zhang, H., 2016. DEM/CFD-DEM modelling of non spherical particulate systems: theoretical developments and applications. Powder Technol. 302, 108–152. https://doi.org/10.1016/j.powtec.2016.07.010.
- Zhu, H.P., Zhou, Z.Y., Yang, R.Y., Yu, A.B., 2008. Discrete particle simulation of particulate systems: a review of major applications and findings. Chem. Eng. Sci. 63 (23), 5728–5770. https://doi.org/10.1016/j.ces.2008.08.006.